Synthesis, Structures, and Solution Dynamics of Functionalized Phosphinomethanide Complexes of the Alkali Metals

M. N. Stuart Hill, Keith Izod,* Paul O'Shaughnessy, and William Clegg

Department of Chemistry, University of Newcastle upon Tyne, Newcastle upon Tyne, NE1 7RU, U.K.

Received May 30, 2000

Metathesis between $[Li\{(Me_3Si)_2C\}P(C_6H_4\text{-}2\text{-}CH_2NMe_2)_2]$ and $NaOBu^t$ in ether yields the sodium phosphinomethanide $[Na\{(Me_3Si)_2C\}P(C_6H_4\text{-}2\text{-}CH_2NMe_2)_2(Et_2O)_{0.5}(DME)_{0.5}]$ (**2b**) after recrystallization. Complex **2b** and its Li and K analogues are highly fluxional in solution, and the dynamic processes accounting for this have been studied by variable-temperature ^1H NMR spectroscopy.

It is well known that the presence of heteroatoms such as Si or P α to a carbanion center acts to increase the stability of that carbanion through hyperconjugation and/or polarization effects.[1] Over the last two decades a substantial number of alkali metal complexes of silicon- and/or phosphorus-stabilized carbanions have been isolated and structurally characterized.[2−5] The structures adopted by these complexes are markedly dependent on the steric and electronic properties of the substituents at phosphorus and/or carbon and on the presence of coligands such as THF or tmeda (tmeda = *N*,*N*,*N*′,*N*′-tetramethylethylenediamine). In particular, the valence isoelectronic, directly bonded P and C centers in phosphinomethanide ligands are able to compete as nucleophiles for coordination to metal centers, leading to a variety of potential bonding modes.[3−5]

We recently reported that incorporation of additional functionality at the periphery of phosphinomethanide ligands can have a dramatic effect on the way in which these ligands bind to alkali metal cations.[5] We now describe the synthesis of a novel amino-functionalized tertiary phosphine and the synthesis and structural characterization of a sodium complex of the phosphinomethanide ligand obtained by its deprotonation, the first such sodium phosphinomethanide to be crystallographically characterized.

Results and Discussion

Treatment of $(Me_3Si)_2CHPCl_2$ with 2 equiv of $Li(C_6H_4\text{-}2\text{-}CH_2NMe_2)$ in cold ether/THF yields the novel tertiary phosphine **1**, according to eq 1, in good yield and purity:

$$(Me_3Si)_2CHPCl_2 + 2[Li(C_6H_4\text{-}2\text{-}CH_2NMe_2)] \xrightarrow{Et_2O/THF(0\ °C)} \{(Me_3Si)_2CH\}P(C_6H_4\text{-}2\text{-}CH_2NMe_2)_2\ (\mathbf{1}) + 2LiCl \quad (1)$$

Metalation of **1** with Bu^nLi, followed by metathesis with $NaOBu^t$, yields the sodium phosphinomethanide **2** as a yellow solid, according to eq 2.

$$[Li\{(Me_3Si)_2C\}P(C_6H_4\text{-}2\text{-}CH_2NMe_2)_2] + NaOBu^t \xrightarrow{Et_2O} [Na\{(Me_3Si)_2C\}P(C_6H_4\text{-}2\text{-}CH_2NMe_2)_2(Et_2O)]\ (\mathbf{2a}) + LiOBu^t \quad (2)$$

Single crystals of the sodium complex were obtained from a cold ether/DME solution as the adduct $[Na\{(Me_3Si)_2C\}P(C_6H_4\text{-}2\text{-}CH_2NMe_2)_2(Et_2O)_{0.5}(DME)_{0.5}]$ (**2b**) (DME = 1,2-dimethoxyethane). Complex **2b** is the first example of a sodium phosphinomethanide to be crystallographically characterized and represents one of only a very few complexes in which there is a genuine contact between sodium and a tertiary phosphine center. The ligand binds the sodium atom through its two amino groups and its phosphorus atom in a PN_2-coordination mode (Figure 1). The coordination sphere of sodium is

* Corresponding author. E-mail: k.j.izod@ncl.ac.uk.

(1) (a) Edwards, G. L. In *Comprehensive Organic Functional Group Transformations*; Katritzky, A. R., Meth-Cohn, O., Rees, C. W., Eds.; Elsevier: Oxford, 1995; pp 579−627. (b) Maryanoff, B. E.; Reitz, A. B. *Chem. Rev.* **1989**, *89*, 863. (c) Römer, B.; Gatev, G. G.; Zhong, M.; Brauman, J. I. *J. Am. Chem. Soc.* **1998**, *120*, 2919. (d) Schleyer, P. von R.; Clark, T.; Kos, A. J.; Spitznagel, G. W.; Rohde, C.; Arad, D.; Houk, K. N.; Rondan, N. G. *J. Am. Chem. Soc.* **1984**, *106*, 6467.

(2) For recent reviews containing information on Si-stabilized carbanions see: (a) Smith, J. D. *Adv. Organomet. Chem.* **1999**, *43*, 267. (b) Schade, C.; Schleyer, P. von R. *Adv. Organomet. Chem.* **1987**, *27*, 169. (c) Setzer, W.; Schleyer, P. von R. *Adv. Organomet. Chem.* **1985**, *24*, 353. (d) Eaborn, C.; Izod, K.; Smith, J. D. *J. Organomet. Chem.* **1995**, *500*, 89. (e) Willard, P. G. In *Comprehensive Organic Synthesis, Vol. 1*; Trost, B. M., Fleming, I., Eds.; Pergammon Press: New York, 1991; pp 1−47. (f) Weiss, E. *Angew. Chem., Int. Ed. Engl.* **1993**, *11*, 1501.

(3) Izod, K. *Adv. Inorg. Chem.* **2000**, *50*, 33, and references therein.

(4) For examples see: (a) Karsch, H. H. *Russ. Chem. Bull.* **1993**, *42*, 1937. (b) Karsch, H. H.; Zellner, K.; Mikulcik, P.; Lachmann, J.; Muller, G. *Organometallics* **1990**, *9*, 190. (c) Karsch, H. H.; Deubelly, B.; Hofmann, J.; Pieper, U.; Muller, G. *J. Am. Chem. Soc.* **1988**, *110*, 3654. (d) Karsch, H. H.; Grauvogl, G.; Mikulcik, P.; Bissinger, P.; Muller, G. *J. Organomet. Chem.* **1994**, *465*, 65. (e) Karsch, H. H.; Ferazin, G.; Bissinger, P. *Chem. Commun.* **1994**, 505. (f) Clegg, W.; Izod, K.; McFarlane, W.; O'Shaughnessy, P. *Organometallics* **1998**, *17*, 5231. (g) Denmark, S. E.; Swiss, K. A.; Wilson, S. R. *Angew. Chem., Int. Ed. Engl.* **1996**, *35*, 2515. (h) Cramer, C. J.; Denmark, S. E.; Miller, P. C.; Dorow, R. L.; Swiss, K. A.; Wilson, S. R. *J. Am. Chem. Soc.* **1994**, *116*, 2437.

(5) (a) Clegg, W.; Doherty, S.; Izod, K.; O'Shaughnessy, P. *Chem. Commun.* **1998**, 1129. (b) Clegg, W.; Izod, K.; O'Shaughnessy, P. *Organometallics* **1999**, *18*, 2939.

10.1021/om000447g CCC: $19.00
Publication on Web 09/23/2000

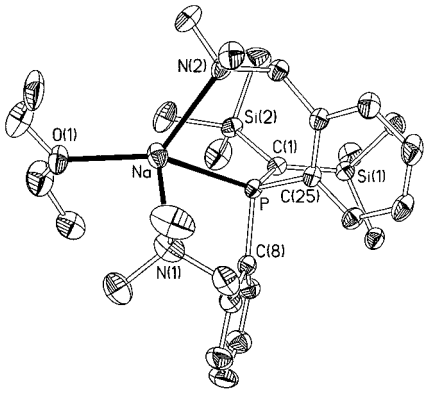

Figure 1. Molecular structure of **2b** with 40% probability ellipsoids and with H atoms omitted for clarity. In the disordered ligand position, diethyl ether is shown and not DME. Selected bond lengths (Å) and angles (deg.): Na−P 2.8004(10), Na−N(1) 2.470(2), Na−N(2) 2.5463(19), Na−O(1) 2.285(3), Na−O(2) 2.429(4), Na−O(3) 2.449(4), P−C(1) 1.750(2), P−C(8) 1.864(2), P−C(25) 1.8589(19), C(1)−Si(1) 1.824(2), C(1)−Si(2) 1.816(2), Si−C(Me) 1.885 (average), N(2)−Na−P 83.39(5), N(1)−Na−P 86.69(6), N(1)−Na−N(2) 115.15(7), N(2)−Na−O(1) 127.32(11), N(2)−Na−O(2) 155.66-(11), N(2)−Na−O(3) 100.63(11), N(1)−Na−O(1) 94.75(11), N(1)−Na−O(2) 89.00(10), N(1)−Na−O(3) 105.63(11), O(2)−Na−O(3) 68.04(13).

completed by contacts to the oxygen atom(s) of diethyl ether or DME, each of which has 50% occupancy in the crystal, and thus achieves a coordination number of four or five. The carbanion center is almost perfectly planar (sum of angles about C(1) = 358.9°), and there is no contact between this center and the sodium atom.

The Na−P distance of 2.8004(10) Å is at the shorter end of the range of reported Na−P distances;[3] in the secondary phosphide complex [Na{([Me_3Si]$_2$CH)P(C_6H_4-2-CH_2NMe_2)}(tmeda)],[6] in which the negative charge of the ligand is localized on phosphorus, the Na−P distance is 2.8396(9) Å. The Na−P distances in the few crystallographically characterized examples of sodium complexes with tertiary phosphine centers are 3.056(2) Å in [Na{$Ph_2P(C_5H_4)$}(DME)]$_2$,[7] 2.852(2) Å in [Na{Pr^i_2-PC(H)═C(O)Ph}]$_4$,[8] and 2.946(6) Å in [Na{(PhCH)Ph_2-PCHPPh_2}(OEt_2)(THF)].[9] Indeed, the only Na−P contact shorter than that observed in **2b** is found in the cluster [EtSi{PNa(SiPr^i_3)}$_3$]$_2$(toluene)$_2$, which has Na−P distances ranging from 2.778(2) to 3.357(2) Å.[10] The short Na−P distance in **2b** is consistent with significant charge delocalization from the carbanion center to phosphorus and the formation of two six-membered chelate rings. The Na−N distances of 2.470(2) and 2.5463(19) Å fall within the range of distances typically found for tertiary amine-complexed sodium atoms.[11]

As was observed in the crystal structures of Li{(Me_3-Si)$_2$C}P(C_6H_4-2-CH_2NMe_2)$_2$] (**3**)[5a] and [K{(Me_3Si)$_2$C}-P(C_6H_4-2-CH_2NMe_2)$_2$]$_n$ (**4**),[5b] the chelate rings of **2b** are puckered such that the benzylic carbon of each chelate ring is oriented in opposite directions with respect to the P−Na vector, leading to an extended pseudo-chair conformation for the two chelate rings. This conformation places one of the aromatic rings side-on to the other, such that the dihedral angle between the planes of the two aromatic rings is 67.8°.

Scheme 1

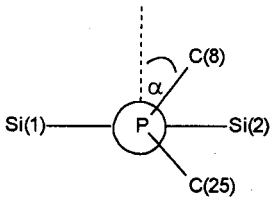

3 α = 3.3 deg.
2b α = 13.2 deg.
4 α = 19.9 deg.

Comparison of the bond lengths and angles within the phosphinomethanide ligands in **2b**, **3**,[5a] and **4**,[5b] all of which possess similar core structures, reveals subtle differences associated with changes in the size and/or polarizability of the metal center. As the cation is changed from Li to Na or K, the P−C(1) distance increases slightly [P−C(1) = 1.735(3), 1.750(2), and 1.752(1) Å, for **3**, **2b**, and **4**, respectively]. This is associated with an increasing deviation from planarity of C(1) [displacement of C(1) from the P−Si(1)−Si(2) plane = 0.0831 Å (Li), 0.1089 Å (Na), 0.1360 Å (K)]. These changes are consistent with reduced multiple-bond character in the P−C(1) bond due to less efficient negative hyperconjugation from the carbanion center to phosphorus. This arises from a twisting of the PAr_2 group with respect to the CSi_2 plane, as measured by an increase in the torsion angle α between the normal to the Si_2P plane (i.e., the direction of the p_z-type lone pair on C(1)) and the P−C(8) vector, as the cation is changed from Li to K [α = 3.3° (**3**), 13.2° (**2b**), 19.9° (**4**)] (Scheme 1 shows a Newmann projection along the P−C(1) bond for **2b**, **3**, and **4**). Such twisting inevitably leads to reduced overlap between the p_z-type lone pair on C(1) and the P−C(Ar) σ^*-orbitals of the PAr_2 group and, thus, to less effective hyperconjugation and a longer P−C(1) bond. These geometrical changes are probably enforced by the increased size of the cation on going from Li to Na or K. Differences in the polarizing ability of the cations may also have an effect on the extent of negative hyperconjugation: the highly polarizing, charge-localizing Li cation may encourage more effective charge delocalization from C(1) to P, in comparison with the larger, less polarizing and more highly coordinated Na and K cations, thus decreasing the P−C(1) distance and enforcing a smaller twist angle α.

The $^{31}P\{^1H\}$ NMR spectrum of **2b** in toluene-d_8 consists of an extremely broad singlet (line width ∼160 Hz) at −7.0 ppm, this line broadening possibly arising from coupling to the quadrupolar ^{23}Na nucleus; in THF-d_8, however, the ^{31}P signal is a sharp singlet at −10.3 ppm, consistent with modulation of the $^{31}P-^{23}Na$ coupling by rapid, reversible P−Na dissociation. Similarly, $^{31}P-^{7}Li$ coupling is resolved for solutions of **3** in toluene-d_8, even at elevated temperatures, but is not resolved in THF-d_8 solutions, even at 213 K.

The room-temperature ^{1}H NMR spectra of complex **2b** in both toluene-d_8 and THF-d_8 solutions are extremely broad. In toluene-d_8 the $SiMe_3$ groups exhibit two broad signals at 0.4 and 0.8 ppm and the NMe_2 groups give rise to a single, extremely broad signal at

(6) Clegg, W.; Doherty, S.; Izod, K.; Kagerer, H.; O'Shaughnessy, P.; Sheffield, J. M. *J. Chem. Soc., Dalton Trans.* **1999**, 1825.
(7) Lin, G.; Wong, W.-T. *Polyhedron* **1994**, *13*, 3027.
(8) Fryzuk, M. D.; Gao, X.; Rettig, S. J. *Can. J. Chem.* **1995**, *73*, 1175.
(9) Schmidbaur, H.; Deschler, U.; Zimmer-Gasse, B.; Neugebauer, D.; Schubert, U. *Chem. Ber.* **1980**, *113*, 902.
(10) Driess, M.; Huttner, G.; Knopf, N.; Pritzkow, H.; Zsolnai, L. *Angew. Chem., Int. Ed. Engl.* **1995**, *34*, 316.
(11) For examples see refs 2a and 2c.

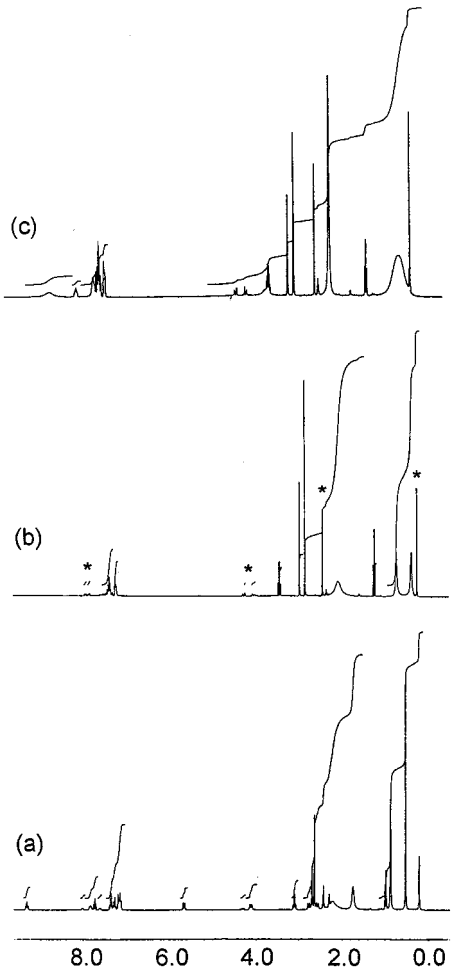

Figure 2. ^{1}H NMR spectra of **2b** in toluene-d_8 at (a) 213 K, (b) 298 K, and (c) 340 K (* free ligand **1**).

approximately 2.0 ppm (Figure 2b). Integration of the aromatic region of the spectrum reveals that the overlapping resonances in this area are due to only four protons; no further signals are evident. As the temperature is raised, the $SiMe_3$ signals coalesce to a single peak, while the NMe_2 signal sharpens considerably. At the highest temperature we were able to obtain (340 K) broad signals due to the CH_2N and the remaining aryl protons are evident at approximately 3.4 and 8.3 ppm, respectively (Figure 2c).

As the temperature is reduced below ambient, the signals due to the $SiMe_3$ groups sharpen considerably; the signal due to the NMe_2 protons separates into two and at 213 K consists of two clearly resolved but still broad peaks (Figure 2a). At this temperature the CH_2N and aryl resonances are also clearly resolved; the former consist of two pairs of doublets at 5.35/2.44 ppm ($^1J_{HH}$ = 12 Hz) and 3.80/2.27 ppm ($^1J_{HH}$ = 10 Hz), while the latter consist of at least six fairly well resolved resonances, indicating that the two chelating arms of the ligand are chemically inequivalent at low temperature. At the lowest temperature we were able to attain (183 K) the NMe_2 protons are clearly resolved as four broad signals. The diastereotopic nature of the methyl substituents of the NMe_2 groups clearly indicates that both amino groups are bound to sodium at this temperature. The low-temperature spectrum of **2b** in d_8-toluene is thus consistent with the structure determined crystallographically; differences between similar atoms on the two chelate rings arise solely from their conformational preferences. The proton *ortho* to the P−C(aryl) bond of one aromatic ring lies close to the other ring, while the equivalent *ortho* proton of the other ring lies in close proximity to the p_z-type lone pair of the carbanion center. This causes the latter proton to resonate at unusually high field (9.02 ppm) and accounts for the wide chemical shift range observed for the aromatic protons. A similar conformational effect accounts for the extremely large chemical shift differences observed between the benzylic protons at low temperature.

The variable-temperature ^{1}H NMR spectra of **3** in toluene-d_8 follow a similar pattern (^{1}H NMR spectra of **4** could not be obtained in toluene-d_8 due to its poor solubility in this solvent). A similar set of variable-temperature ^{1}H NMR spectra are obtained for **2b**, **3**, and **4** in THF-d_8.

Fluxionality in complexes with benzylamine-type ligands has been observed for a range of metal and nonmetal centers.[12−15] In particular, van Koten et al. and Reich et al. have reported detailed NMR studies of several such complexes, including 2-[(dimethylamino)-methyl]phenyllithium (**5**).[13,14] A recent investigation into the fluxional behavior of ^{15}N−^{6}Li doubly labeled **5** suggests that chelation by the NMe_2 groups persists in THF solution below −55 °C; a monomer−dimer equilibrium exists above −55 °C, and intermolecular exchange causes signal averaging.[14] This suggests that any Na−N cleavage in **2b** should be frozen out at low temperatures and thus that its structure in THF-d_8 solution at low temperature is likely to be similar to that in the solid state. The similarities in the low-temperature NMR spectra of **2b** in toluene-d_8 and THF-d_8 are also consistent with this compound adopting a similar structure in both solvents.

Calculation of the activation parameters $\Delta G^{\ddagger}$, $\Delta H^{\ddagger}$, and $\Delta S^{\ddagger}$ by line shape analysis of the $SiMe_3$ and NMe_2 regions of the ^{1}H NMR spectra of **2b**, **3**, and **4** in THF-d_8 and of **2b** and **3** in toluene-d_8 reveals several interesting trends (the behavior of the NMe_2 protons is taken to be representative of the behavior of the chelating arms of the ligands); a summary of these parameters is given in Table 1.

The similarity between the activation parameters for **2b** and **3** in toluene-d_8 suggests that the same dynamic processes are in operation for these two complexes in this solvent. However, the NMe_2 and $SiMe_3$ groups

(12) For examples see: (a) Gruter, G.-J. M.; van Klink, G. P. M.; Akkerman, O. S.; Bickelhaupt, F. *Chem. Rev.* **1995**, *95*, 2405, and references therein. (b) Jastrzebski, J. T. B. H.; van Koten, G.; Tuck, D. G.; Meinema, H. A.; Noltes, J. G. *Organometallics* **1982**, *1*, 1492. (c) Osman, A.; Steevensz, R. G.; Tuck, D. G.; Meinema, H. A.; Noltes, J. G. *Can. J. Chem.* **1984**, *62*, 1698. (d) Klumpp, G. W.; Vos, M.; de Kanter, F. J. J. *J. Am. Chem. Soc.* **1985**, *107*, 8292.

(13) (a) Wehman, E.; Jastrzebski, J. T. B. H.; Ernsting, J.-M.; Grove, D. M.; van Koten, G. *J. Organomet. Chem.* **1988**, *353*, 145. (b) Wijkens, P.; van Koten, E. M.; Janssen, M. D.; Jastrzebski, J. T. B. H.; Spek, A. L.; van Koten, G. *Angew. Chem., Int. Ed. Engl.* **1995**, *34*, 219. (c) Wijkens, P.; Jastrzebski, J. T. B. H.; Veldman, N.; Spek, A. L.; van Koten, G. *Chem. Commun.* **1997**, 2143. (d) Hüls, D.; Günther, H.; van Koten, G.; Wijkens, P.; Jastrzebski, J. T. B. H. *Angew. Chem., Int. Ed. Engl.* **1997**, *36*, 2629.

(14) Reich, H. J.; Gudmundsson, B. Ö. *J. Am. Chem. Soc.* **1996**, *118*, 6074.

(15) (a) Toyota, S.; Futawaka, T.; Ikeda, H.; Oki, M. *Chem. Commun.* **1995**, 2499. (b) Toyota, S.; Oki, M. *Bull. Chem. Soc. Jpn.* **1991**, *64*, 1554. (c) Toyota, S.; Futuwaka, T.; Asakura, M.; Ikeda, H.; Oki, M. *Organometallics* **1998**, *17*, 4155. (d) Schlengermann, R.; Sieler, J.; Jelonek, S.; Hey-Hawkins, E. *Chem. Commun.* **1997**, 197.

Table 1. Activation Parameters for the Dynamic Processes Observed by ^{1}H NMR Spectroscopy for 2b, 3, and 4 in Toluene-d_8 and THF-d_8

		toluene-d_8				THF-d_8			
complex	group	T_c[a]	$\Delta G^{\ddagger}$[b]	$\Delta H^{\ddagger}$[c]	$\Delta S^{\ddagger}$[d]	T_c[a]	$\Delta G^{\ddagger}$[b]	$\Delta H^{\ddagger}$[b]	$\Delta S^{\ddagger}$[d]
3	$SiMe_3$	296	55	51	−29	274	52	26	−108
	NMe_2	343	67	46	−75	284	54	29	−101
2b	$SiMe_3$	293	56	44	−48	263	50	36	−63
	NMe_2	336	65	44	−71	273	52	35	−70
4	$SiMe_3$					263	51	53	−3
	NMe_2					269	51	37	−67

[a] Coalescence temperature (K). [b] At T_c in kJ mol^{-1} (±3). [c] kJ mol^{-1} (±3). [d] J K^{-1} mol^{-1} (±10).

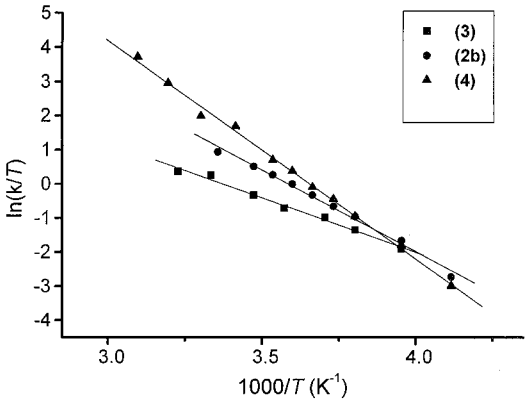

Figure 3. Plot of ln(k/T) vs $1/T$ for the NMe_2 region of **2b**, **3**, and **4** in THF-d_8.

within each complex appear to be subject to (substantially) independent dynamic processes for which values of $\Delta H^{\ddagger}$ are similar but values of $\Delta S^{\ddagger}$ are quite different.

In THF-d_8 the values of $\Delta G^{\ddagger}$ for both the $SiMe_3$ and NMe_2 groups are essentially identical ($\Delta G^{\ddagger} = 50-54$ kJ mol^{-1}), irrespective of the metal. For **2b** and **3** in THF-d_8 the values of $\Delta H^{\ddagger}$ and $\Delta S^{\ddagger}$ for the process affecting the $SiMe_3$ group are, within experimental error, identical to the values of these parameters for the process affecting the NMe_2 groups, suggesting that the same dynamic process is responsible for the coalescence of both sets of peaks. For **4** there is a significant difference in the values of $\Delta H^{\ddagger}$ and $\Delta S^{\ddagger}$ for the process(es) affecting the $SiMe_3$ and NMe_2 groups. The activation parameters obtained in THF-d_8 for **2b** and **3** differ considerably from those obtained in toluene-d_8, suggesting that different dynamic processes might operate in these two solvents.

A plot of ln(k/T) vs $1/T$ for the NMe_2 or $SiMe_3$ groups of **2b**, **3**, and **4** in THF-d_8 on the same axes shows a reasonably clear isokinetic point (Figure 3). This suggests that the same structure is adopted by all three complexes in this solvent and confirms that the same dynamic process is in operation; differences in molecular architecture seen in the solid state are not significant in the solution phase.[16]

The dynamic processes responsible for the fluxionality of the chelating arms of the ligands may be based in two separate effects: changes in chelate ring conformation (mechanism ***Ia***, Scheme 2) and/or reversible dissociation of the NMe_2 groups or P-center from the alkali metal (mechanism ***Ib***). Mechanism ***Ia*** results in complete interconversion of the protons on chelate ring A

Scheme 2

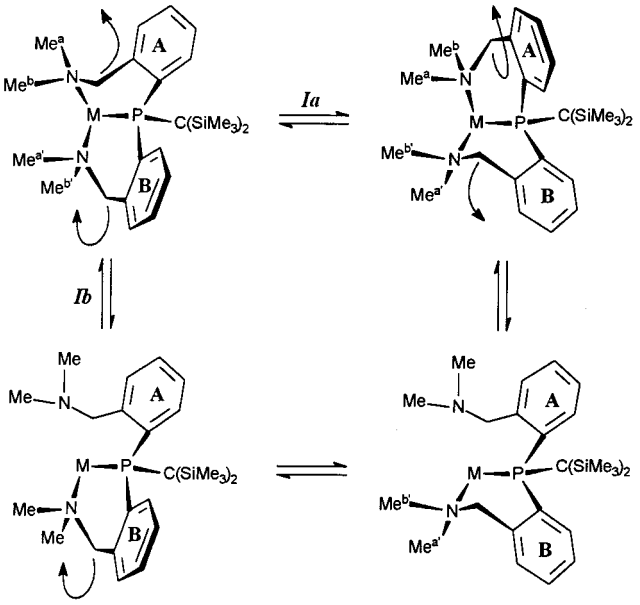

with those on chelate ring B without interconverting the methyl groups attached to the same nitrogen. Mechanism ***Ib***, however, will render both the two chelating arms and the two methyl groups (Me^a and Me^b) on the same nitrogen equivalent on the NMR time scale. Similarly, reversible P−M cleavage would lead to equivalence of the protons on both arms of the ligand on the NMR time scale, but not to equivalence of Me^a and Me^b (for clarity only M−N cleavage is illustrated in Scheme 2). M−N/M−P dissociation would simultaneously have the effect of relieving steric congestion about the $SiMe_3$ groups, allowing rotation about the P−C(1) bond and thus making these groups equivalent at high temperatures.

The poor donor ability of toluene, combined with the stability associated with a bis-chelate ligand and the large negative entropy of activation for the process affecting the NMe_2 groups in **2b** and **3**, suggests that mechanism ***Ib*** is unlikely to be responsible for the dynamic behavior of the chelating arms of the ligands in toluene-d_8. The $SiMe_3$ groups appear to be subject to a different dynamic process than the NMe_2 groups in toluene-d_8, which we attribute to restricted rotation about the P−C(1) bond due to a combination of steric hindrance and multiple P−C bond character caused by negative hyperconjugation.

The strong, hard O-donor ligand THF is much more likely than toluene to displace the phosphinomethanide donor groups from the hard alkali metal cations, and thus in THF-d_8 it is more likely that the dynamic process responsible for the high-temperature equivalence of the two chelating arms of the ligand is due to mechanism ***Ib***, in which M−N or M−P dissociation is accompanied by coordination of the metal center by THF. The large negative entropy of activation for this process is indicative of a large degree of ordering in the transition state, consistent with an associatively led substitution of a chelating NMe_2 group or phosphorus center by THF.

Clearly it is not possible to distinguish unambiguously between mechanisms ***Ia*** and ***Ib***, and it may be that the observed fluxionality is due to a combination of these

(16) Isaacs, N. S. *Physical Organic Chemistry*, 2nd ed.; Longman: London, 1995; pp 116−118.

two processes. In particular, it is difficult to distinguish between M−N and M−P cleavage in mechanism ***Ib***, although the lack of $^{7}Li-^{31}P$ coupling in THF-d_8 for **3**, even at low temperatures, and the mismatch between the hard alkali metal cations and soft P-center suggest that P−M cleavage might play a role.

Conclusions

The heavier alkali metal phosphinomethanide complex [Na{$(Me_3Si)_2C$}$P(C_6H_4$-2-$CH_2NMe_2)_2(Et_2O)_{0.5}$-$(DME)_{0.5}$] (**2b**) is readily accessible by a simple metathesis route. Variation in the size and polarizing ability of the cation in **2b**, **3**, and **4** causes subtle changes in the bond lengths and angles within the phosphinomethanide ligands, associated with a decrease in P−C multiple-bond character on going from Li to Na to K.

Although the available data do not allow us to draw definitive conclusions regarding the dominant mechanism accounting for the fluxionality of **2b**, **3**, and **4** in solution, it appears that different dynamic processes are responsible for the fluxionality of the $SiMe_3$ groups and the chelating arms of the ligands of **2b** and **3** in toluene-d_8. The chelating arms of the ligands are most likely subject to a conformational change, whereas the $SiMe_3$ groups are subject to a restricted rotation about the P−C(1) bond due to steric hindrance and P−C multiple-bond character. In THF-d_8 it appears that the same dynamic process is responsible for the fluxionality of the $SiMe_3$ groups as is responsible for the fluxionality of the chelating arms of the ligands in all three complexes and that this process is different from those that operate in toluene-d_8. We propose that the dominant process in this case involves either reversible M−N or M−P cleavage and subsequent conformational changes in the chelating arms of the ligands.

Experimental Section

General Comments. All manipulations were carried out using standard Schlenk techniques under an atmosphere of dry nitrogen or argon. Ether, THF, DME, and light petroleum (bp 40−60 °C) were distilled from potassium or sodium/potassium alloy under an atmosphere of dry nitrogen and stored over a potassium film (with the exception of THF and DME, which were stored over activated 4 Å molecular sieves). Deuterated benzene, toluene, and THF were distilled from potassium and were deoxygenated by three freeze−pump−thaw cycles and stored over activated 4 Å molecular sieves. Li[C_6H_4-2-CH_2NMe_2],[17] [Li{$(Me_3Si)_2C$}$P(C_6H_4$-2-$CH_2NMe_2)_2$] (**3**),[5a] and {$(Me_3Si)_2CH$}PCl_2[18] were prepared according to previously published procedures. $NaOBu^t$ was purchased from Aldrich and dried by heating under vacuum (100 °C/10^{-2} mmHg) for 4 h before use. Bu^nLi was purchased from Acros Organics as a 2.5 M solution in hexanes.

^{31}P and ^{23}Na NMR spectra were recorded on a Bruker WM300 spectrometer operating at 121.5 and 79.4 MHz, respectively, and ^{1}H and ^{13}C spectra on a Bruker AC200 spectrometer, operating at 200.1 and 50.3 MHz, respectively. ^{1}H and ^{13}C chemical shifts are quoted in ppm relative to tetramethylsilane; ^{31}P chemical shifts are quoted relative to external 85% H_3PO_4; ^{23}Na chemical shifts are quoted relative to external 5% NaCl in H_2O. Elemental analyses were obtained by Elemental Microanalysis Ltd., Okehampton, U.K.

Preparation of {$(Me_3Si)_2CH$}$P(C_6H_4$-2-$CH_2NMe_2)_2$ (1). To a cold (0 °C) solution of {$(Me_3Si)_2CH$}PCl_2 (3.18 g, 13 mmol) in ether (20 mL) was added, dropwise, a solution of Li[C_6H_4-2-CH_2NMe_2] (3.52 g, 26 mmol) in THF (30 mL). This mixture was allowed to attain room temperature and was stirred for 2 h. Solvent was removed in vacuo, and the oily residue was extracted into light petroleum (40 mL) and filtered. Solvent was removed from the filtrate in vacuo to give **1** as a colorless oil. Yield: 4.13 g, 69%. Anal. Calcd for $C_{25}H_{43}N_2PSi_2$: C, 65.45; H, 9.45; N, 6.11. Found: C, 64.96; H, 9.92; N, 6.00. ^{1}H NMR (C_6D_6): δ 0.03 (18 H, s, $SiMe_3$), 1.34 (1 H, d, J_{PH} = 4.5 Hz, CHP), 2.18 (12 H, s, NMe_2), 3.78 (2 H, d, $^{1}J_{HH}$ = 14 Hz, CH_2N), 4.03 (2 H, dd, $^{1}J_{HH}$ = 14 Hz, $^{3}J_{PH}$ = 3.4 Hz, CH_2N), 7.03 (2 H, m, ArH), 7.11 (2 H, m, ArH), 7.62 (2 H, s, ArH), 7.68 (2 H, m, ArH). $^{13}C\{^{1}H\}$ NMR (C_6D_6): δ 3.12 ($SiMe_3$), 12.07 (d, J_{PC} = 51.6 Hz, CHP), 46.23 (NMe_2), 62.75 (d, J_{PC} = 24.9 Hz, CH_2N), 127.17, 129.18, 129.84, 134.00 (Ar), 140.59 (d, J_{PC} = 21.7 Hz, Ar), 144.34 (d, J_{PC} = 25.9 Hz, Ar). ^{31}P NMR (C_6D_6): δ −46.5.

Preparation of [{$(Me_3Si)_2C$}$P(C_6H_4$-2-$CH_2NMe_2)_2$]Na-$(OEt_2)_{0.5}(DME)_{0.5}$ (2b). A solution of **3** (1.29 g, 2.78 mmol) in diethyl ether (10 mL) was added to a suspension of $NaOBu^t$ (0.28 g, 2.78 mmol) in the same solvent (15 mL). The reaction mixture was stirred for 12 h, and then solvent was removed in vacuo. The solid was washed with light petroleum (bp 40−60 °C, 3 × 10 mL), and the resulting powder was recrystallized from ether containing a few drops of DME as irregular yellow plates of **2b**. Yield: 1.06 g, 68%. Anal. Calcd for $C_{29}H_{52}N_2$-$NaO_{1.5}PSi_2$: C, 61.88; H, 9.31; N, 4.98. Found: C, 59.61; H, 8.67; N, 5.23. ^{1}H NMR (THF-d_8, 213 K): δ −0.47 (s, 9 H, $SiMe_3$), 0.01 (s, 9 H, $SiMe_3$), 1.10 (t, 3 H, Et_2O), 1.98 (s, 6 H, NMe_2), 2.31 (s, 6 H, NMe_2), 2.88 (d, $^{2}J_{HH}$ = 14.8 Hz, 1 H, CH_2N), 3.35 (q, 2 H, Et_2O), 3.53 (dd, $^{2}J_{HH}$ = 14.8 Hz, J_{PH} = 6.4 Hz, 1 H, CH_2N), 3.97 (d, $^{2}J_{HH}$ = 15.6 Hz, 1 H, CH_2N), 4.27 (dd, $^{2}J_{HH}$ = 15.6 Hz, J_{PH} = 6.4 Hz, 1 H, CH_2N), 6.56 (m, 1 H, *p*-ArH_B), 6.68 (m, 1 H, *m*-ArH_B), 6.81 (m, 1 H, *m*-ArH_B), 6.91 (m, 1 H, *p*-ArH_A), 7.03 (m, 1 H, *m*-ArH_A), 7.34 (m, 1 H, *m*-ArH_A), 7.37 (m, 1 H, *o*-ArH_B), 8.28 (m, 1 H, *o*-ArH_A). $^{31}P\{^{1}H\}$ NMR (THF-d_8, 297 K): δ −10.3. ^{23}Na NMR (THF-d_8 297 K): δ 3.4.

Crystal Structure Determination of 2b. Data were collected at 160 K on a Bruker AXS SMART CCD diffractometer with graphite-monochromated Mo Kα radiation (λ = 0.71073 Å). Crystal data: $C_{29}H_{52}N_2NaO_{1.5}PSi_2$, M = 562.9, monoclinic, space group $P2_1/c$, a = 17.0866(16) Å, b = 11.4896(11) Å, c = 18.9224(18) Å, β = 114.909(2)°, V = 3369.3(6) Å^3, Z = 4, D_{calcd} = 1.110 g cm^{-3}, μ = 0.19 mm^{-1}, crystal size 0.48 × 0.36 × 0.26 mm; structure solution by direct methods, refinement on F^2 for all 8133 unique absorption-corrected data (2θ < 28.8°); $R_w = \{\sum[w(F_o^2 - F_c^2)^2]/\sum[w(F_o^2)^2]\}^{1/2}$ = 0.1218 (all data), conventional R = 0.0493 on F values of 4847 reflections with $F_o^2 > 2\sigma(F_o^2)$, goodness of fit = 0.922, final difference synthesis within ±0.54 e Å^{-3}. Programs: Bruker AXS SMART (diffractometer control), SAINT (data integration), and SHELXTL (structure solution and refinement).

Acknowledgment. This work was supported by the EPSRC and The Royal Society. The authors thank Prof. W. McFarlane for helpful discussions regarding NMR spectra.

Supporting Information Available: For **2b** details of structure determination, atomic coordinates, bond lengths and angles, and displacement parameters. This material is available free of charge via the Internet at http://pubs.acs.org. Observed and calculated structure factor details are available from the authors upon request.

OM000447G

(17) Jastrzebski, J. T. B. H.; van Koten, G. *Inorg. Synth.* **1989**, *26*, 150.

(18) Gynane, M. J. S.; Hudson, A.; Lappert, M. F.; Power, P. P.; Goldwhite, H. *J. Chem. Soc., Dalton Trans.* **1980**, 2428.